Astronomy
&
Astrophysics

Dielectronic recombination data for dynamic finite-density plasmas

VI. The boron isoelectronic sequence

Z. Altun[1], A. Yumak[1], N. R. Badnell[2], J. Colgan[3], and M. S. Pindzola[3]

[1] Department of Physics, Marmara University, Istanbul, 81040, Turkey
[2] Department of Physics, University of Strathclyde, Glasgow G4 0NG, UK
[3] Department of Physics, Auburn University, Auburn, AL 36849, USA

Abstract. We have calculated dielectronic recombination rate coefficients for 22 ions of the boron isoelectronic sequence, between C^+ and Xe^{49+}, within the generalized collisional-radiative framework, as outlined by Badnell et al. (2003). Calculations have been performed from both ground and metastable initial states, in both LS- and intermediate-coupling, allowing for $\Delta n = 0$ and $\Delta n = 1$ core-excitations. Results are presented and discussed for a selection of ions from the sequence. Results which are not presented here can be accessed from the Atomic Data and Analysis Structure (ADAS) database (Summers 2003) or from the Oak Ridge Controlled Fusion Atomic Data Center (`http://www-cfadc.phy.ornl.gov`). Comparison is made with the results of other existing theoretical calculations.

Key words. atomic data – atomic processes – plasmas

1. Introduction

The programme to generate a total and final-state level-resolved intermediate-coupling dielectronic recombination database necessary for the spectroscopic modelling of dynamic finite-density plasmas, where the coronal approximation is not valid, has been described by Badnell et al. (2003). To this end, results have been calculated for dielectronic recombination data from the ground plus metastable initial states of the isoelectronic sequences of lithium (Colgan et al. 2004), beryllium (Colgan et al. 2003), carbon (Zatsarinny et al. 2004) and oxygen (Zatsarinny et al. 2003). In this paper, we present results for dielectronic recombination data for the boron isoelectronic sequence. Boron-like ions are present in a variety of astrophysical objects such as novae, planetary nebulae, Seyfert galaxies, the interstellar medium and the Sun. Thus, accurate atomic data is needed not only for the spectral diagnostics of laboratory plasmas but also for the diagnostics of these important astrophysical objects. Since the pioneering work by Burgess (1964, 1965), much effort has been spent, both theoretically and experimentally, to obtain accurate dielectronic recombination rate coefficients for many atomic ions. Results of many of these studies have been summarized and compiled by a

number of workers – see Shull & van Steenberg (1982), Arnaud & Rothenflug (1985), and Mazzotta et al. (1998). There have been many previous calculations of dielectronic recombination for the boron-like ions, most of which present only total recombination rates from the ground state without considering the metastable initial states. Here, we present final-state level-resolved recombination rates from the ground plus metastable initial states. It is noted that both $\Delta n = 0$ and $\Delta n = 1$ core-excitations are important for highly-charged ions, and also that radiative stabilization of the spectator electron can contribute significantly to dielectronic recombination.

Dielectronic recombination rate coefficients for Fe^{21+} were calculated by Badnell (1986) using a multi-configuration LS-coupling expansion, allowing for $\Delta n = 0$ and $\Delta n = 1$ core-excitations, at temperatures between 10^5 and 10^9 K. Badnell and Pindzola (1989) have carried-out LS- and intermediate-coupling calculations for dielectronic recombination rate coefficients of C^+, N^{2+}, and O^{3+} ions, between 10^4 and 10^7 K, allowing only for $\Delta n = 0$ core-excitations from the ground state. Dielectronic recombination cross sections for N^{2+}, O^{3+} and F^{4+} were estimated by Nasser & Hahn (1989) using single configuration non-relativistic Hartree-Fock wave functions in LS-coupling, over an incident electron energies ranging from 0.07 to 1.15 Ryd. Badnell et al. (1991) have calculated energy-averaged dielectronic recombination cross sections in

LS-coupling from the ground and metastable initial states of O^{3+} and F^{4+} ions, as a function of electron energy ranging from 0 to 25 eV. There was an early calculation on C^+ by LaGattuta and Hahn (1983) in *LS*-coupling in the range of 9.0 to 9.3 eV using *LS* term-averaged Hartree-Fock single-particle states in a frozen-core approximation. Zhang and Pradhan (1997) have carried-out calculations on Fe^{21+} using a relativistic Breit-Pauli formulation of the R-matrix method in a close coupling approximation, including the radiation damping of autoionizing resonances. Studies for the total recombination rate coefficients of boron-like ions from carbon to aluminum have been carried-out by Nahar (1995) and Nahar & Pradhan (1997) within a close coupling approximation using the R-matrix method, which are in good agreement with earlier results for low-*T* dielectronic recombination rate coefficients of Nussbaumer & Story (1983) and the high-*T* dielectronic recombination rate coefficients of Jacobs et al. (1979). Dielectronic recombination rate coefficients for boron-like Ar^{13+} have been calculated by Chen et al. (1998) within the multi-configuration Dirac-Fock method for electron temperatures between 0.1 and 10^4 eV. Mazzotta et al. (1998) have compiled tables of fits of total dielectronic recombination rate coefficients from these references for all ions of the elements He to Ni in the zero electron density limit. Recently, calculations for dielectronic recombination rate coefficients of all K-shell and L-shell H- to Ne-like ions of seven elements, namely Mg, Si, S, Ar, Ca, Fe, and Ni, have been made by Gu (2003) using a fully-relativistic factorized distorted-wave approximation. In this paper we compare our results with those of several of these more recent data compilations.

An early experiment on C^+ by Mitchel et al. (1983) was carried-out over a very narrow energy range between 9.04 to 9.32 eV. The first measurements of dielectronic recombination cross sections on N^{2+}, O^{3+}, and F^{4+} ions were made by Dittner et al. (1988) involving the $2s \rightarrow 2p$ transition. These measurements were found to be consistent with theoretical calculations done in the same paper in an isolated resonance distorted-wave approximation by Hahn and Nasser. Calculations of dielectronic recombination for O^{3+} and F^{4+} ions by Badnell et al. (1991) using a mixed target state, including $\Delta n = 0$ and $\Delta n = 1$ core-excitations, described quite well the experimental results of the Aarhus group (see Badnell et al. 1991). Measurements for the dielectronic recombination of Ar^{13+} between 0.2 and 6.0 eV by DeWitt et al. (1995) were found to be in good agreement with the calculations by Badnell (see DeWitt et al. 1996) within the multi-configuration Breit-Pauli approximation. Recent accurate measurements of dielectronic recombination resonance strengths and energies for Fe^{21+} forming Fe^{20+} via $n = 2 \rightarrow 2$ ($\Delta n = 0$) core-excitations were carried-out by Savin et al. (2003).

The current work presents multi-configuration intermediate-coupling Breit-Pauli (MCBP) calculations of final-state level-resolved dielectronic recombination rate coefficients for all ions in the boron-like isoelectronic sequence up to Ar^{13+}, as well as Ca^{15+}, Ti^{17+}, Cr^{14+}, Fe^{21+}, Ni^{23+}, Zn^{25+}, Kr^{31+}, Mo^{39+}, and Xe^{49+}. As previously discussed (Badnell et al. 2003) this data will form part of the Atomic Data and Analysis Structure (ADAS) database comprising the data files for each ion, detailing the rate coefficients to each *LS* and *LS J*-resolved final-state from both ground and metastable initial states. This is available though the ADAS project (Summers 2003) and is also available on-line at the Oak Ridge Controlled Fusion Atomic Data Center (`http://www-cfadc.phy.ornl.gov`).
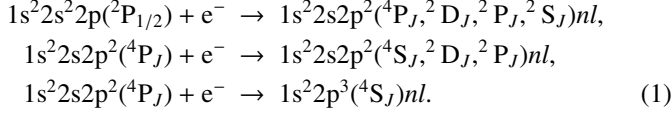
The effect of weak external electric fields on the high Rydberg states which frequently dominate the dielectronic recombination process was discussed by Burgess & Summers (1969). The effect of the plasma microfield on dielectronic recombination was studied by Jacobs et al. (1976). Recent experimental (Bartsch et al. 1997) and theoretical (Robicheaux & Pindzola 1997; Griffin et al. 1997; Mitnik et al. 1999) studies have shown the importance of the effects of crossed external electric and magnetic fields. However, as explained by Badnell et al. (1993, 2003), field-free data is the most suitable starting point for plasma modelling.

The main goal of this work is to calculate multi-configuration intermediate-coupling dielectronic recombination rate coefficients from the ground plus metastable initial states of an ion to all possible final states, in an appropriate form for generalized collisional-radiative modelling. The final-state level-resolved dielectronic recombination rate coefficients are important for the collisional-radiative modelling of dense plasmas. The dielectronic recombination rate coefficients associated with metastable states is particularly needed for modelling dynamic plasmas, since the metastable states (and the populations built upon them) are not in quasi-static equilibrium with the ground state. Calculations have been carried-out over a wide range of electron temperatures, $Z^2(10^1-10^7)$ K where Z is the target ion charge, for a range of boron-like ions from C to Xe. Results are presented in both *LS*- and intermediate-coupling approximations. Our intermediate-coupling MCBP results were found to be in good agreement with other existing measurements and calculations over electron temperatures ranging from $\sim Z^2(10^2-10^7)$ K. In Sect. 2 we give a brief description of the theory used and in Sect. 3 we present some dielectronic recombination rate coefficients for selected ions in the boron isoelectronic sequence and compare them with the results of other workers. We conclude with a brief summary.
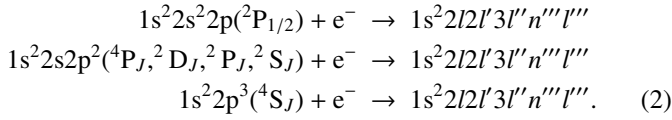
2. Theory

The theoretical details of our calculations have already been described in detail (Badnell et al. 2003). Here we outline only the main points. The AUTOSTRUCTURE code (Badnell 1986, 1997; Badnell & Pindzola 1989) was used to calculate energy levels, radiative and autoionization rates in the *LS*- and intermediate-coupling multi-configuration Breit-Pauli (MCBP) approximations using non-relativistic (up to Zn) and semi-relativistic (from Zn) radial functions. The autoionization rates are calculated in the isolated resonance approximation using distorted waves. This enables the generation of final-state level-resolved and total dielectronic recombination rate coefficients in the independent processes approximation, i.e. we neglect interference between the radiative recombination and the dielectronic recombination processes. Although this has been found to be only a very small effect for the total rate (Pindzola et al. 1992), more recent studies of partial recombination cross

sections for Li-like fluorine, F^{6+}, (Mitnik et al. 1999) predict some interference between these processes for weak partial cross sections. The dielectronic capture process for boron-like ions can be represented, in intermediate-coupling, for $\Delta n = 0$ core-excitations, by

$$1s^2 2s^2 2p(^2P_{1/2}) + e^- \rightarrow 1s^2 2s 2p^2(^4P_J,{}^2D_J,{}^2P_J,{}^2S_J)nl,$$
$$1s^2 2s 2p^2(^4P_J) + e^- \rightarrow 1s^2 2s 2p^2(^4S_J,{}^2D_J,{}^2P_J)nl,$$
$$1s^2 2s 2p^2(^4P_J) + e^- \rightarrow 1s^2 2p^3(^4S_J)nl. \tag{1}$$

In this case, l and n values were included up to 15 and a quantum-defect approximation for high-level values of n up to 1000 were used (Badnell et al. 2003). For $\Delta n = 1$ core-excitations the dielectronic capture process can be written as

$$1s^2 2s^2 2p(^2P_{1/2}) + e^- \rightarrow 1s^2 2l2l'3l''n'''l'''$$
$$1s^2 2s 2p^2(^4P_J,{}^2D_J,{}^2P_J,{}^2S_J) + e^- \rightarrow 1s^2 2l2l'3l''n'''l'''$$
$$1s^2 2p^3(^4S_J) + e^- \rightarrow 1s^2 2l2l'3l''n'''l'''. \tag{2}$$

Similarly, values of l' up to $l' = 6$ were included along with values of n up to $n = 15$. Again an approximation for the high-level values of n was used up to $n = 1000$.

The dielectronic recombination rate coefficient from an initial metastable state ν to a final-state i is given by

$$\alpha_{i\nu}^{z+1} = \left(\frac{4\pi a_0^2 I_H}{k_B T_e} \right)^{3/2} \sum_j \frac{\omega_j}{2\omega_\nu} e^{-E_c/k_B T_e}$$
$$\times \frac{\sum_l A_{j\rightarrow\nu,E_c l}^a A_{j\rightarrow i}^r}{\sum_h A_{j\rightarrow h}^r + \sum_{m,l} A_{j\rightarrow m,E_c l}^a}, \tag{3}$$

where ω_j is the statistical weight of the $(N+1)$-electron doubly-excited resonance state j, ω_ν is the statistical weight of the N electron target state and the autoionization (A^a) and radiative (A^r) rates are in inverse seconds. Here, E_c is the energy of the continuum electron of angular momentum l, which is fixed by the position of the resonances, and I_H is the ionization potential energy of the hydrogen atom, k_B is the Boltzmann constant, T_e is the electron temperature and $(4\pi a_0^2)^{3/2} = 6.6011 \times 10^{-24}$ cm^3. Calculations were carried out within the independent processes and isolated resonance approximations using the AUTOSTRUCTURE computer code which is implemented within the ADAS suite of programs as ADAS701. For $\Delta n = 0$ core-excitations, the resonance energies are empirically adjusted so that the series limits match the 2−2 excitation energies obtained from the NIST evaluated database (http://physics.nist.gov/). Accurate resonance energies are particularly important for the calculations of low-temperature dielectronic recombination rate coefficients. Separate calculations are done for the different core-excitations ($\Delta n = 0$ and $\Delta n = 1$). Separate calculations were also made for the different parities. Finally, LS- and intermediate-coupling dielectronic recombination rate coefficients for different core-excitations were saved under common file names to be added to the existing ADAS database.

3. Results

Numerical results, obtained in both LS- and intermediate-coupling and for both $\Delta n = 0$ and $\Delta n = 1$ core-excitations, are available on the web (http://www-cfadc.phy.ornl.gov). They provide final-state level-resolved dielectronic recombination rate coefficients from both the ground and metastable initial states into final LS terms or LSJ levels in a manner useful to fusion and astrophysical modellers. We have used the formula

$$\alpha = \frac{1}{T^{3/2}} \sum_{i=1}^5 c_i e^{-E_i/T} \tag{4}$$

to fit all of our intermediate-coupling results so as to facilitate the use of our data by others. In this equation, T and E_i have units of Kelvin and the rate coefficients α have units of cm^3/s. Our fits are accurate to better than 5% for all ions in the temperature range $Z^2(5 \times 10^3 – 10^7)$ K, where Z is the residual charge of the initial ion, except for C^+ where the fit is only good down to 2×10^4 K. In Table 1 we present a list of total dielectronic recombination rate coefficients, c_i and E_i, for each member of the boron isoelectronic sequence considered. These fitting coefficients have been obtained from the sum of the dielectronic recombination rate coefficients calculated separately for $\Delta n = 0$ and $\Delta n = 1$ core-excitations.

We first compare our intermediate-coupling MCBP results for dielectronic recombination rate coefficients for Fe^{21+} forming Fe^{20+} via $2 \rightarrow 2$ ($\Delta n = 0$) core-excitations with measurements carried-out using the heavy-ion Test Storage Ring at the Max-Planck-Institute for Nuclear Physics in Heidelberg, Germany by Savin et al. (2003). We have used the experimental energy spread of Savin et al. (2003) associated with the relative motion between the ions and the electrons, corresponding to temperatures $k_B T_\perp = 14$ meV perpendicular to the confining magnetic field and $k_B T_\parallel = 0.15$ meV parallel to the magnetic field, in the convolution of our results. We included all possible $1s^2 2s^2 2pnl$, $1s^2 2s 2p^2 nl$, and $1s^2 2p^3 nl$ resonance configurations with $2 \le n \le 1000$ and $0 \le l \le 25$, and all corresponding continuum configurations $1s^2 2s^2 2p\epsilon l$, $1s^2 2s 2p^2 \epsilon l$, and $1s^2 2p^3 \epsilon l$ associated with the target states $1s^2 2s^2 2p$, $1s^2 2s 2p^2$, and $1s^2 2p^3$. To account for field ionization effects we also eliminated all resonances with $n > 116$. Prior to the final dielectronic recombination cross section calculations, the calculated ionic thresholds were shifted to the known spectroscopic values taken from the NIST evaluated data for atomic energy levels by amounts varying between 0.9 eV and 4.0 eV.

A Slater-Type-Orbital model potential was used to generate the radial orbitals. The same optimum form was used for the whole isoelectronic sequence. Configuration mixing was within the boron-like ground complex only. The 4.0 eV shift is the worst case and refers only to the $1s^2 2p^3(^4S)$ level. Levels of the $1s^2 2s 2p^2$ configuration were shifted between 1.0 and 2.6 eV, mostly less than 2.0 eV, and the upper $1s^2 2s^2 2p$ level by 0.9 eV, all relative to the ground state. We have also added intermediate-coupling non-resonant radiative recombination contributions, convolved with the same energy spread, to dielectronic recombination so as to facilitate comparison with experiment since it does not distinguish between the two. As can be seen from the comparison of the experimental results of Savin et al. (2003) in Fig. 1a with our theoretical results in Fig. 1b, our intermediate-coupling MCBP calculations reproduce all of the main resonances fairly well, except for the

Table 1. Fitting coefficients c_i and E_i for Eq. (5), for ions in the boron isoelectronic sequence. All coefficients refer to our intermediate-coupling calculations obtained on using non-relativistic (up to Zn) and semi-relativistic (from Zn) radial functions.

Ion	$c1$	$c2$	$c3$	$c4$	$c5$	$E1$	$E2$	$E3$	$E4$	$E5$
C^{1+}	1.320(−4)	1.536(−3)	⋯	⋯	⋯	7.767(+4)	1.445(+5)	⋯	⋯	⋯
N^{2+}	2.852(−6)	2.527(−3)	2.660(−3)	3.831(−5)	⋯	1.138(+4)	1.568(+5)	2.734(+5)	2.207(+6)	⋯
O^{3+}	7.373(−5)	6.993(−3)	3.848(−3)	⋯	⋯	2.421(+4)	2.156(+5)	5.280(+5)	⋯	⋯
F^{4+}	7.484(−5)	4.107(−4)	1.106(−2)	7.752(−3)	5.428(−5)	1.524(+4)	8.531(+4)	2.690(+5)	7.860(+5)	2.663(+7)
Ne^{5+}	1.008(−4)	4.468(−4)	1.286(−2)	3.594(−3)	3.682(−5)	4.434(+3)	5.551(+4)	2.864(+5)	5.488(+5)	2.065(+7)
Na^{6+}	2.428(−5)	2.370(−4)	8.724(−4)	1.738(−2)	4.006(−4)	2.663(+3)	1.725(+4)	7.876(+4)	3.366(+5)	7.301(+5)
Mg^{7+}	7.061(−5)	3.888(−4)	1.280(−3)	2.018(−2)	6.917(−3)	3.967(+2)	1.801(+4)	1.090(+5)	3.606(+5)	8.175(+5)
Al^{8+}	4.154(−4)	4.693(−3)	2.758(−2)	8.932(−2)	2.491(−4)	2.523(+4)	1.499(+5)	4.840(+5)	2.119(+6)	9.967(+7)
Si^{9+}	7.523(−4)	3.044(−3)	2.935(−2)	3.142(−2)	1.043(−1)	6.213(+3)	5.519(+4)	4.265(+5)	1.605(+6)	2.727(+6)
P^{10+}	2.365(−3)	9.402(−3)	3.563(−2)	1.834(−1)	8.211(−4)	1.251(+4)	2.215(+5)	6.480(+5)	2.980(+6)	1.148(+8)
S^{11+}	3.045(−4)	6.254(−3)	4.378(−2)	1.273(−1)	1.354(−1)	1.007(+4)	1.372(+5)	5.574(+5)	2.864(+6)	3.937(+6)
Cl^{12+}	1.840(−3)	8.373(−3)	4.678(−2)	2.500(−1)	8.666(−2)	2.481(+4)	1.364(+5)	6.117(+5)	3.521(+6)	5.151(+6)
Ar^{13+}	3.891(−3)	9.335(−3)	5.181(−2)	1.756(−1)	2.515(−1)	2.623(+4)	1.476(+5)	6.510(+5)	3.453(+6)	5.201(+6)
Ca^{15+}	2.670(−3)	1.376(−2)	6.014(−2)	1.447(−1)	4.960(−1)	3.285(+4)	1.904(+5)	7.015(+5)	3.358(+6)	6.221(+6)
Ti^{17+}	9.883(−3)	4.257(−2)	9.323(−2)	8.194(−1)	5.463(−3)	4.518(+4)	3.766(+5)	1.425(+6)	6.902(+6)	7.176(+7)
Cr^{19+}	1.713(−2)	2.134(−2)	9.576(−2)	2.308(−1)	9.005(−1)	3.466(+4)	1.581(+5)	7.964(+5)	4.244(+6)	9.014(+6)
Fe^{21+}	9.625(−3)	2.866(−2)	1.204(−1)	3.762(−1)	1.038(+0)	6.220(+3)	1.519(+5)	8.770(+5)	5.386(+6)	1.104(+7)
Ni^{23+}	2.165(−2)	9.738(−2)	1.631(−1)	1.391(+0)	1.828(−1)	7.919(+4)	5.695(+5)	2.332(+6)	1.049(+7)	1.974(+7)
Zn^{25+}	8.799(−3)	4.532(−2)	1.624(−1)	3.706(−1)	1.574(+0)	4.481(+3)	1.952(+5)	1.068(+6)	5.663(+6)	1.399(+7)
Kr^{31+}	5.410(−2)	2.348(−1)	4.048(−1)	2.324(+0)	1.150(−1)	1.506(+5)	9.217(+5)	4.926(+6)	1.818(+7)	4.375(+7)
Mo^{37+}	1.856(−2)	1.699(−1)	4.146(−1)	1.124(+0)	2.418(+0)	4.227(+4)	4.532(+5)	2.171(+6)	1.216(+7)	2.904(+7)
Xe^{49+}	3.379(−2)	3.724(−1)	8.706(−1)	1.742(+0)	2.886(+0)	9.613(+4)	7.842(+5)	4.172(+6)	2.014(+7)	4.925(+7)

low-lying resonances just above threshold where the results are quite sensitive to small energy differences in resonance positions. This agreement for Fe^{21+} is encouraging for our systematic study of boron-like ions from C to Xe.

In Fig. 2 we compare our intermediate-coupling MCBP Maxwell-averaged final-state level-resolved dielectronic recombination rate coefficients for Fe^{+21} as a function of electron temperature with those of the recent calculations of Gu (2003), who used a fully-relativistic factorized distorted-wave approximation. As can be seen, there is no practical difference between our intermediate-coupling results and those of Gu. Our LS-coupling results are included to emphasize the importance of relativistic effects in these calculations, particularly at low electron temperatures. The fitting data provided for Fe^{21+} by Mazzotta et al. (1998) agrees with both our results and those of Gu only for higher electron temperatures. The comparison of intermediate-coupling MCBP dielectronic recombination rate coefficients, for only the $n = 2 \rightarrow 2$ ($\Delta n = 0$) core-excitations, with those of Savin et al. (2003) shows excellent agreement over the entire range of electron temperature.

Figure 3 shows the final-state level-resolved dielectronic recombination rate coefficients for C^+, calculated within the intermediate-coupling approximation, from the initial $2s^2 2p$ $^2P_{1/2}$ level to the final-state levels $2s^2 2p^2$ $^3P_{0,1,2}$, $2s^2 2p^2$ $^1D_2$, $2s^2 2p^2$ $^1S_0$, and $2s2p^3$ $^5S_0$. Of course, there exist hundreds of final-state levels for this ion alone, for which final-state level-resolved dielectronic recombination rate coefficients may be obtained from the ADAS database.

Figure 4 shows the present LS- and intermediate-coupling total dielectronic recombination rate coefficients as functions of temperature for O^{3+}. The comparison of our results with

the fitting data of Mazzotta et al. (1998) shows good agreement over the entire range of electron temperature above 10^4 K. Mazzotta et al. (1998) obtained their fitting data for boron-like ions from a compilation of works, viz. Nussbaumer & Storey (1983) for C to Al, Jacobs et al. (1979) for Si to S, and Arnaud & Rothenflug (1985) for Fe. They used the general formula of Burgess (1965) with some corrections by Merts et al. (1976) for ions for which results were not available. Contributions from $2 \rightarrow 2$ $\Delta l = 0$ fine-structure transitions to dielectronic recombination are missing from both our LS-coupling results and earlier ones used in the fitting data of Mazzotta et al. This explains the discrepancy between our intermediate-coupling results and those of Mazzotta et al. and our LS-coupling results, below 10^4 K.

In Fig. 5 we compare our results for LS- and intermediate-coupling total dielectronic recombination rate coefficients for Ne^{5+} with the results obtained from the tables of Mazzotta et al. (1998). These results are in quite good agreement over all electron temperatures, except for the region between temperatures 10^4 and 10^5 K.

In Fig. 6a we present total dielectronic recombination rate coefficients for Si^{9+}. We compare our LS- and intermediate-coupling results with the results obtained from the tables of fits of Mazzotta et al. (1998). Our results are also compared with the results of recent calculations by Gu (2003). Our intermediate-coupling results are in excellent agreement with those of both Mazzotta and Gu over all electron temperatures. Our LS-coupling results differ from these somewhat at temperatures below 10^3 K and this difference is due to the contributions from fine-structure core-excitation channels that are not accounted-for by an LS-coupling calculation. Figure 6b
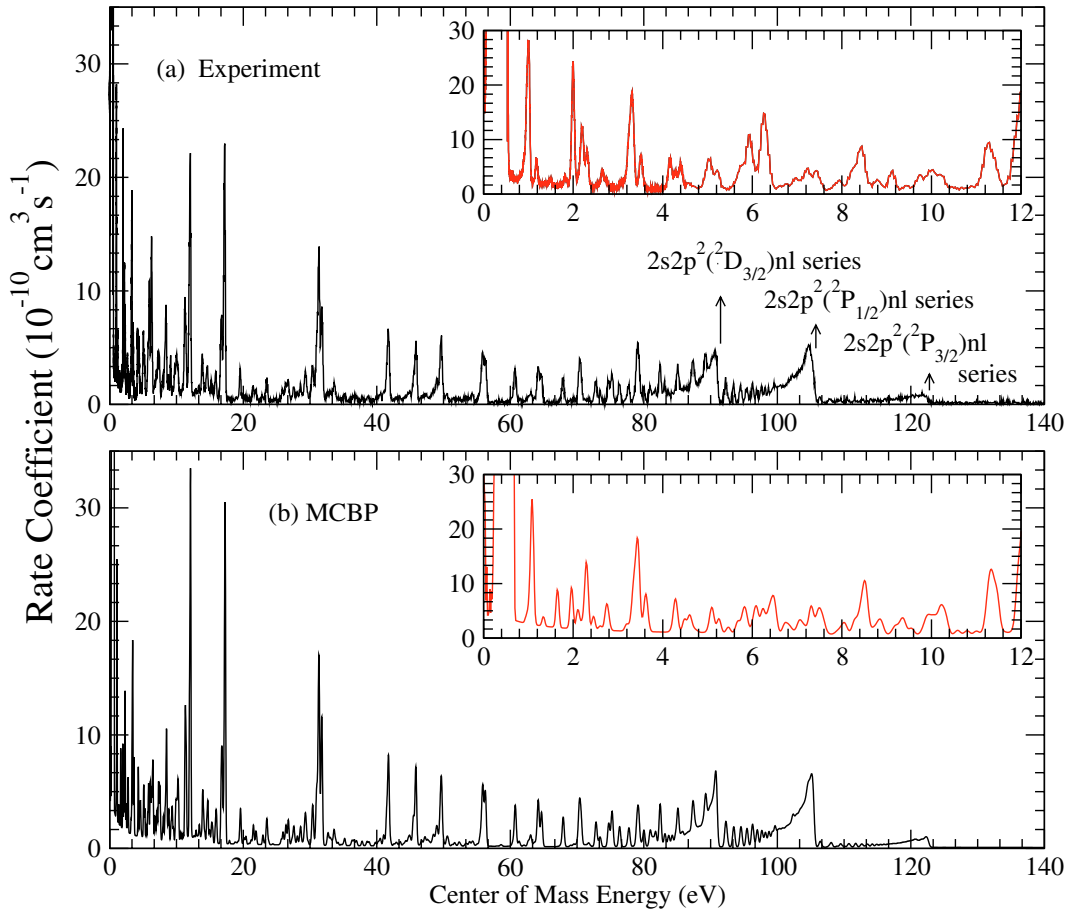
Fig. 1. Resonance structure for Fe^{21+} forming Fe^{20+} via $n = 2 \rightarrow 2$ ($\Delta n = 0$) core-excitations. **a)** Experimental results (Savin et al. 2003); **b)** intermediate-coupling MCBP results. Expanded views of these resonances are also shown.

compares separately our intermediate-coupling dielectronic recombination rate coefficients for $\Delta n = 0$ and $\Delta n = 1$ core-excitations with those of Gu (2003). The results are in excellent agreement for the entire electron temperature range. The agreement is also an indication of the fact that contributions from inner-shell excitations, i.e. from the 1s shell, are quite small, since such excitations are not included in the current calculations but are included in the calculations of Gu (2003).

In Fig. 7 we present total dielectronic recombination rate coefficients for Ca^{15+}. We compare both of our total *LS*- and intermediate-coupling results with those of Mazzotta et al. (1998) and Gu (2003). In both cases, our results are in excellent agreement with those of Gu (2003) over a wide range of electron temperatures. However, results obtained from the tables of fits of Mazzotta et al. (1998) differ significantly from both the current results and those of Gu below 10^5 K. Slight differences between the current results and those of Gu below 10^4 K may be attributed to slight differences in the energy positions of the low-lying resonances.

We have presented results for a selection of boron-like ions, all of which show good agreement with the results of recent calculations by Gu (2003), obtained within a fully-relativistic factorized distorted-wave approximation. This type of good agreement is also found for ions for which results are not

presented here explicitly, but are made available through the ADAS project (Summers 2003).

4. Summary

We have carried-out systematic calculations of dielectronic recombination data for the boron-like isoelectronic sequence as part of an assembly of a dielectronic recombination database necessary for the modelling of dynamic finite-density plasmas (Badnell et al. 2003). Calculations were carried-out in a multi-configuration intermediate-coupling Breit-Pauli approximation for all ions up to Ar^{13+}, as well as Ca^{15+}, Ti^{17+}, Cr^{14+}, Fe^{21+}, Ni^{23+}, Zn^{25+}, Kr^{31+}, Mo^{39+}, and Xe^{49+} using non-relativistic (up to Zn) and semi-relativistic (from Zn) radial functions.

The good agreement between our intermediate-coupling MCBP results and the measurements from the Test Storage Ring in Heidelberg (Savin et al. 2003) for the Fe^{21+} forming Fe^{20+} via $2 \rightarrow 2$ ($\Delta n = 0$) core-excitations is a good indication of the validity of the approximations used in obtaining the results presented in this paper.

We have calculated *LS J* final-state level-resolved dielectronic recombination rate coefficients in a form which will be useful for the modellers of both astrophysical and fusion plasmas. Although our approximations are such that each final-state level-resolved dielectronic recombination rate coefficient
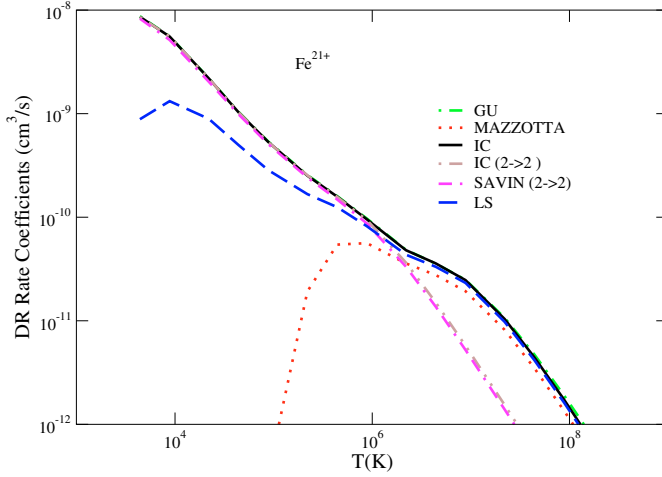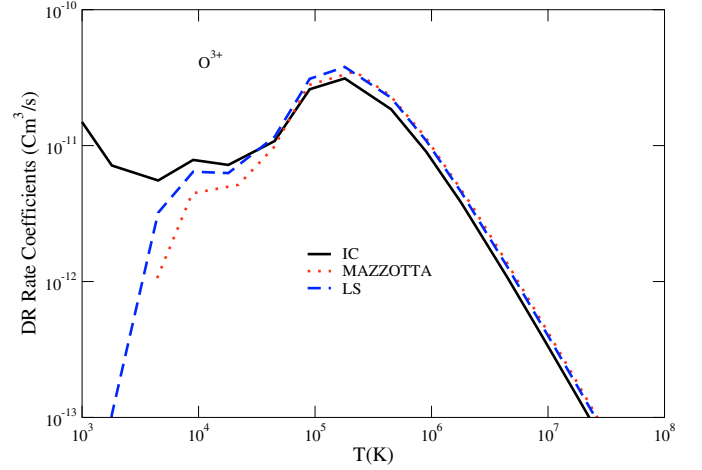
Fig. 2. Total dielectronic recombination rate coefficients for Fe^{21+} to Fe^{20+}, as a function of electron temperature (in Kelvin). The solid curve represents our intermediate-coupling MCBP results. The dotted line (lying just on top of the solid curve) represents the recent fully-relativistic results of Gu (2003). The fitting data of Mazzotta et al. (1998), based on the work of Nussbaumer & Storey (1983), is represented by the dot-dashed line. Our *LS*-coupling configuration-mixed results are represented by the dashed line. The double-dotted-dashed line represents intermediate-coupling MCBP dielectronic recombination rate coefficients, based only on the $n = 2 \rightarrow 2$ ($\Delta n = 0$) core-excitations. The double-dashed-dotted line represents experimentally derived rate coefficients, for just the $n = 2 \rightarrow 2$ core-excitations (Savin et al. 2003).
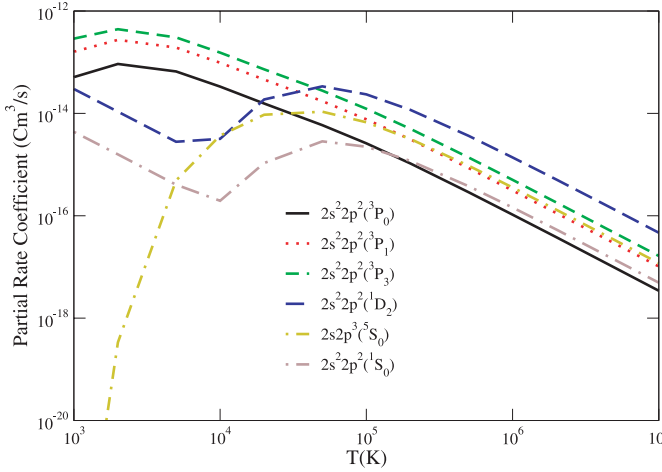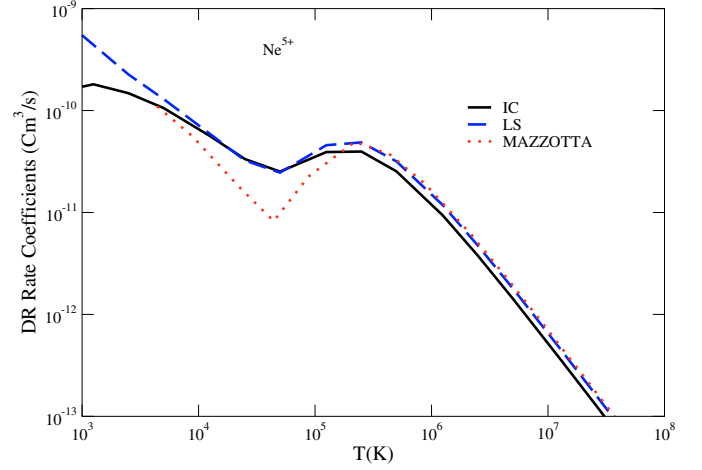

Fig. 3. Final-state level-resolved dielectronic recombination rate coefficients for C^+ as a function of electron temperature (in Kelvin). We present final-state level-resolved rate coefficients from the initial $2s^2 2p\ ^2P_{1/2}$ level to the final-state levels as indicated (where we have dropped the $1s^2$ part of the configuration for clarity).

may not be as highly accurate as some of the most sophisticated techniques available today, we have calculated a consistent set of data over a wide range of electron temperatures and for a large number of atomic ions in order to maximize the available information for modelling work.

We have presented selected final-state level-resolved and total rate coefficients for some ions of interest and have made comparisons, where possible, with previous works. We have

Fig. 4. Total dielectronic recombination rate coefficients for O^{3+} as a function of electron temperature (in Kelvin). We compare our *LS*- and intermediate-coupling MCBP results with the data adopted by Mazzotta et al. (1998).
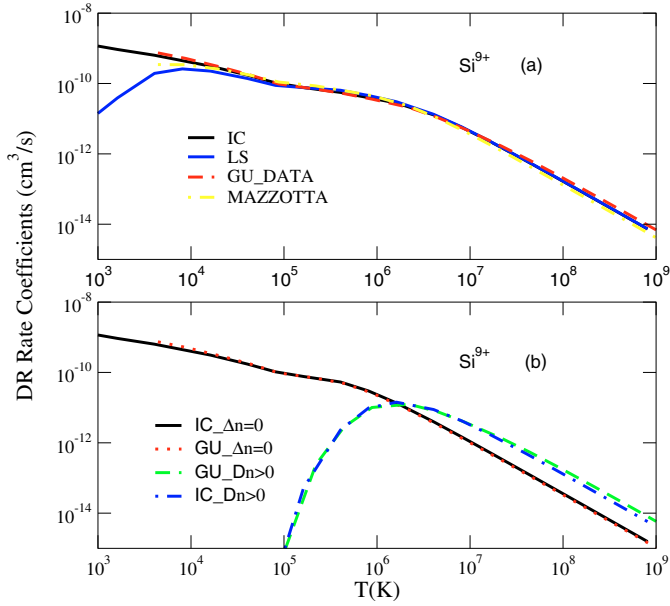

Fig. 5. Total dielectronic recombination rate coefficients for Ne^{5+} as a function of electron temperature (in Kelvin). Our *LS*- and intermediate-coupling MCBP results are compared with the data adopted by Mazzotta et al. (1998).

found particularly large disagreements with the fits from the recent critical compilation of Mazzotta et al. (1998) for the electron temperatures below below $\sim 5 \times 10^5 Z^2$ K. On the other hand, the agreement between our results and those of Gu (2003) was found to be excellent.

Our high-temperature total rate coefficients should be accurate to $\sim 30\%$, for all ions in the temperature range $\sim Z^2 (5 \times 10^3 - 10^7)$ K, since the effects of external electric and magnetic fields are not included in the calculations. In the future we will present dielectronic recombination data for further iso-electronic sequences, as discussed previously (Badnell et al. 2003).

Fig. 6. a) Total dielectronic recombination rate coefficients; and **b)** separate contributions from the $\Delta n = 0$ and $\Delta n = 1$ core-excitations, for for Si^{9+} as a function of electron temperature (in Kelvin). We compare our configuration mixed LS- and intermediate-coupling MCBP results with the data adopted of Mazzotta et al. (1998), and with the results of recent calculations by Gu (2003).
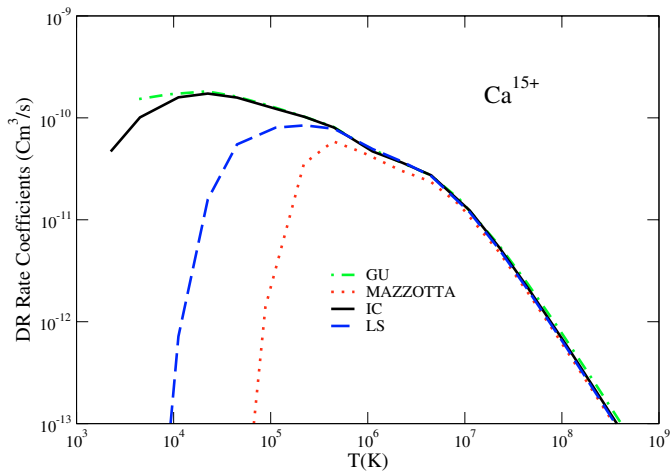
Fig. 7. Dielectronic recombination rate coefficient for Ca^{15+} as a function of electron temperature (in Kelvin). We compare our configuration-mixed LS- and intermediate-coupling MCBP results with the results of data adopted by Mazzotta et al. (1998), and with the results of Gu (2003).

References

Arnaud, M., & Rothenflug, R. 1985, A&AS, 60, 425

Badnell, N. R. 1986, J. Phys. B, 19, 3827

Badnell, N. R. 1997, J. Phys. B, 30, 1

Badnell, N. R., O'Mullane, M., Summers, H. P., et al. 2003, A&A, 406, 1151

Badnell, N. R., & Pindzola, M. S. 1989, Phys. Rev. A, 39, 1685

Badnell, N. R., Pindzola, M. S., Andersen, L. H., Bolko, J., & Schmidt, H. T. 1991, J. Phys. B, 24, 4441

Badnell, N. R., Pindzola, M. S., Dickson, W. J., et al. 1993, ApJ, 407, L91, 4441

Bartsch, T., Schippers, S., Müller, A., et al. 1997, Phys. Rev. Lett., 82, 3779

Burgess, A. 1964, ApJ, 139, 776

Burgess, A. 1965, ApJ, 141, 1588

Burgess, A., & Summers, H. P. 1969, ApJ, 157, 1007

Chen, M. H., Reed, K. J., Guo, D. S., & Savin, D. W. 1998, Phys. Rev. A, 58, 4539

Colgan, J., Pindzola, M. S., Whiteford, A. D., & Badnell, N. R. 2003, A&A, 412, 597

Colgan, J. Pindzola, M. S., & Badnell, N. R. 2004, A&A, 417, 1183

DeWitt, D. R., Schuch, R., Gao, H., et al. 1996, Phys. Rev. A, 53, 2327

Dittner, P. F., Datz, S., Hippler R., et al. 1988, Phys. Rev. A, 38, 2762

Griffin, D. C., Robicheaux, F., & Pindzola, M. S. 1998, Phys. Rev. A, 57, 2708

Gu, M. F. 2003, ApJ, 590, 1131

Jacobs, V. L., Davis, J., & Kepple, P. C. 1976, Phys. Rev. Lett., 37, 1390

Jacobs, V. L., Davis, J., Rogerson J. E., & Blaha, M. 1979, ApJ, 230, 627

Jacobs, V. L., Davis, J., & Blaha, M. 1980, ApJ, 239, 1119

LaGattuta, K., & Hahn, Y. 1983, Phys. Rev. Lett., 50, 668

Merts, A. L., Cowan, R. D., & Magee, J. 1976, Los Alamos Scientific Laboratory Report LA-6220-MS (BM)

Mitchel, J. B. A., Ng, C. T., Forand, J. L., et al. 1983, Phys. Rev. Lett, 50, 335

Mazzotta, P., Mazzitelli, G., Colafrancesco, S., & Vittorio, N. 1998, A&AS, 133, 403

Mitnik, D. M., Pindzola, M. S., & Badnell, N. R. 1999, Phys. Rev. A, 59, 3592

Nahar, S. N. 1995, ApJS, 101, 423

Nahar, S. N., & Pradhan, A. K. 1997, ApJS, 111, 339

Nasser I., & Hahn, Y. 1989, Phys. Rev. A, 39, 401

Nussbaumer, H., & Storey, P. J. 1983, A&A, 126, 75

Pindzola, M. S., & Badnell, N. R. 1992, Nucl. Fusion and Plasma Material Interaction data for fusion, 3, 101

Pindzola, M. S., Badnell, N. R., & Griffin, D. C. 1992, Phys. Rev. A, 46, 5725

Robicheaux, F., & Pindzola, M. S. 1997, Phys. Rev. Lett., 79, 2237

Robicheaux, F., Pindzola, M. S., & Griffin, D. C. 1998, Phys. Rev. Lett., 80, 1402

Savin, D. W., Kahn, S. M., Gwinner, G., et al. 2003, ApJS, 147, 421.

Shull, J. M., & van Steenberg, M. 1982, ApJS, 48, 95

Summers, H. P., 2003, ADAS User Manual (v2.6), available from http://adas.phys.strath.ac.uk/adas/docs/manual

Zhang, H. L., & Pradhan, A. K. 1997, A&AS, 123, 575

Zatsarinny, O., Gorczyca, T. W., Korista, K. T., Badnell, N. R., & Savin, D. W. 2003, A&A, 412, 587

Zatsarinny, O., Gorczyca, T. W., Korista, K. T., Badnell, N. R., & Savin, D. W. 2004, A&A, 417, 1173